A Case Study of a Shunt and Preexisting Series Simultaneous Fault

Eric Johnson
Dominion Energy

Luke Booth and Joe Perigo
Schweitzer Engineering Laboratories, Inc.

Presented at the
79th Annual Conference for Protective Relay Engineers
College Station, Texas
March 30–April 2, 2026

Previously presented at the
78th Annual Georgia Tech Protective Relaying Conference, May 2025

Originally presented at the
26th Annual Georgia Tech Fault and Disturbance Conference, May 2025

A Case Study of a Shunt and Preexisting Series Simultaneous Fault

Eric Johnson, *Dominion Energy*
Luke Booth and Joe Perigo, *Schweitzer Engineering Laboratories, Inc.*

***Abstract*—On August 11th, 2023, a shunt fault occurred on a utility networked line that had a previously existing series fault. The series fault was a missing jumper associated with A-phase, which created an open phase. Because the series fault was preexisting when the shunt fault occurred, both faults existed at the same time. This occurrence is defined as a simultaneous fault. Simultaneous faults are rare, and it can be difficult to discern that they occurred. They produce fault currents and voltages that are a challenge to protective relay elements. This paper analyzes a real-world case study of a simultaneous fault on a transmission system to empower the industry with knowledge of how to discern simultaneous faults from traditional nonsimultaneous faults. The paper describes the fault, the voltages and currents observed during the fault, and the analysis that took place to discover that both a series and shunt fault existed at the same time. The paper further implements a first-principles approach for investigating faulted circuits. This analysis is used to give a description of how a series fault and a shunt fault would have appeared on this system if they had occurred separately, and how this contrasts with the case of a simultaneous fault. This provides the opportunity to compare the analytical approach against the power system response for validation. The paper discusses a corrective action that can be implemented to detect an open-phase fault and, subsequently, prevent simultaneous fault conditions.**

I. Introduction

On August 11th, 2023, a shunt fault occurred on a Dominion Energy South Carolina circuit that had a previously existing series fault. Shunt faults are short-circuit faults. The series fault was a missing jumper associated with A-phase, which created an open phase. Because the series fault was preexisting when the shunt fault occurred, the combination of both faults at the same time is defined as a simultaneous fault [1]. Simultaneous faults are rare, and it can be difficult to discern when they occur. They produce fault currents and voltages that are a challenge to protective relay elements.

This fault occurred on a 33 kV networked circuit on the utilities system. The protective relaying scheme implements the traditional three-pole trip (3PT) scheme. Even though this voltage is not in the range of the bulk electric system, this analysis is pertinent to any networked system. Fig. 1 is a one-line depiction of the system the fault existed in. It is evident that there is a parallel circuit to the circuit that experienced the simultaneous fault. The faulted circuit is termed Line 1 and the parallel circuit Line 2.

The preexisting open phase was present about nine tower spans from Substation A; a jumper on one of the towers was missing on A-phase. How long it had been missing is unknown. Load flow was too low to provide enough unbalance for the ground overcurrent elements to pick up, and no open-phase detection methods were implemented. On August 11th, 2023, an A-phase to C-phase shunt fault occurred closer to the Substation B end of the line. The protective relays protecting Line 1 operated correctly and cleared the fault. The primary protective relay associated with Breaker 3 and associated with Line 2 momentarily saw the fault in a Ground Zone 1 element and instantaneously operated. This was an unnecessary operation because the fault was in the parallel line. This unnecessary operation is what spurred the utility to reach out to the relay manufacturer.

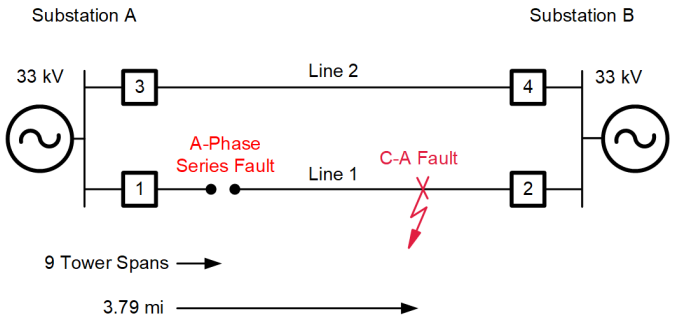

Fig. 1. System one-line diagram.

The first part of this paper describes how initial analysis determined there was an unknown preexisting condition present: the missing jumper creating the series fault. This condition, coupled with the shunt fault, caused voltage and current signals to look nontraditional. This provided clues that, when investigated, uncovered the preexisting series fault. And upon physical inspection, it was discovered that the series fault was still present on the system. This knowledge led the utility to replace the missing jumper, renetworking A-phase on Line 1. The paper continues by providing a few methods to detect the presence of an existing series fault on networked or radial lines to help mitigate an occurrence like this for the utility and others in the future.

The next section of the paper provides readers with an analytical approach for solving both nonsimultaneous and simultaneous faulted circuits. This section starts with a discussion of traditional symmetrical components and contrasts them with the advantages of phase-domain circuit analysis for simultaneous faults. To achieve this, a phase-domain model of the parallel line is developed based on the line parameters of the circuit. A refresher is then given on how the system would have responded if the series fault or the shunt phase-to-phase fault occurred independently of each other. The simultaneous fault is then simulated and compared against the field event report data.

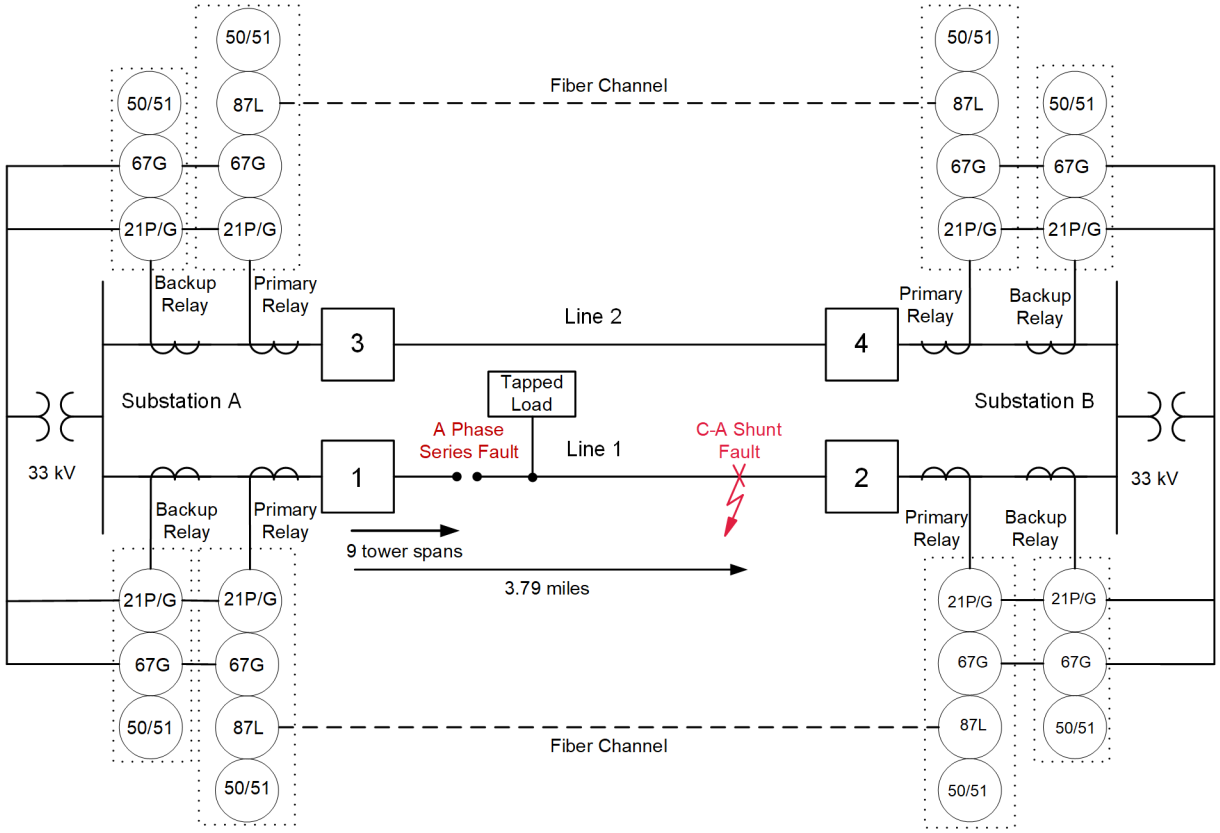

Fig. 2. System one-line diagram with protective relay elements.

II. Initial Root-Cause Analysis

To understand this fault, it is necessary to understand the system it existed in. The system is a networked 33 kV system. In time past, the networked system served load that is no longer present. It remains networked primarily as a contingency to backfeed a 115 kV system. Fig. 2 is a one-line diagram of the system. The bus at Substation A and the bus at Substation B are straight buses. Other breakers are connected to these buses but not shown as they are not necessary for the analysis. The distance between Line 1 and Line 2 is 4.12 miles.

As seen in Fig. 2, both lines have primary and backup protective relays. The primary relay has American National Standards Institute (ANSI) protective elements, 21P, 21G, 50/51, and 87L. The line differential channel is over a direct fiber connection. The backup relay has 21P, 21G, and 50/51 ANSI element protection.

On August 11th, 2023, a phase-to-phase fault occurred from A-phase to C-phase on Line 1. The Breaker 2 relays calculated the fault was 0.33 miles from Substation B, which was verified by the line crew. The Breaker 1 primary relay stated the fault was 9.67 miles away, which would have been incorrect for an in-zone fault on a 4.12-mile line. The Breaker 1 backup relay reported the fault location was 3.22 miles away. This is closer but still .57 miles off from what the Breaker 2 relays estimated. Fig. 3 displays the filtered voltages and currents recorded by the Breaker 1 relays. Fig. 4 displays the filtered voltages and currents recorded by the Breaker 2 relays.

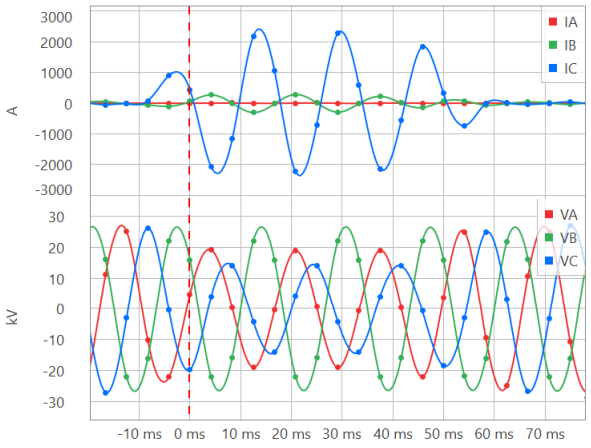

Fig. 3. Filtered voltages and currents of the Breaker 1 relays during the fault.

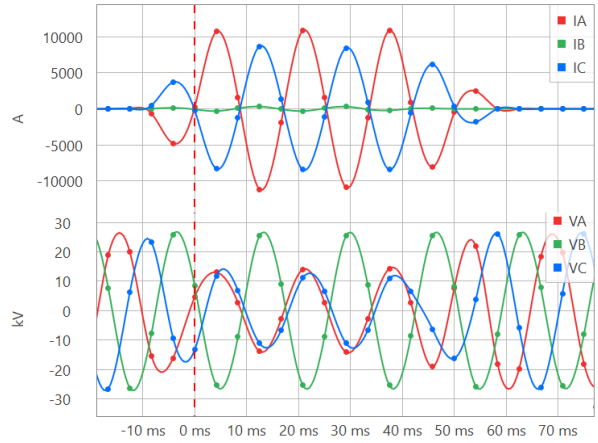

Fig. 4. Filtered voltages and currents of the Breaker 2 relays during the fault.

Initial observations can be made from oscillographs. At Breaker 1, the current oscillography does not look like a traditional phase-to-phase fault involving A- and C-phases. The A-phase current is nonexistent, while the C-phase current is high. The B-phase current increases slightly and, at initial glance, appears to be 180 degrees out of phase from C-phase. But both A-phase and C-phase voltage depress with C-phase depressing more.

At Breaker 2, the current signature more closely resembles a phase-to-phase fault. Both A-phase and C-phase voltages also depress. One would expect though that A-phase voltage would depress more than C-phase since the A-phase current is higher than the C-phase current.

The 87L element between Breaker 1 and Breaker 2 primary protective relays correctly declares this fault as an in-zone fault, and the line is cleared.

During the phase-to-phase fault, the Breaker 3 primary relay identified the fault in its Zone 1 quadrilateral ground element. As a Zone 1 element it was set with no intentional time delay and operated, opening Breaker 3. Because this network is meant for contingency system conditions it did not negatively affect the system or load. The Breaker 4 primary relay triggered an event report based on an overcurrent element detection but did not assert any directional or distance elements. The Breaker 4 secondary relay did not trigger an event report. The line differential element correctly restrained for this out-of-zone fault. Fig. 5 displays the filtered voltages and currents seen by the Breaker 3 relays. Fig. 6 displays the filtered voltages and currents seen by the Breaker 4 primary relay.

Glancing at the Breaker 3 and Breaker 4 oscillographies, the current angles appear to match a phase-to-phase fault but with A-phase current significantly higher than C-phase current. This introduces a significant amount of zero-sequence current. It appears that A-phase and C-phase voltages also resemble a phase-to-phase fault as the phase angle between them seems to reduce. Again, notice that A-phase voltage is higher than C-phase voltage, even though A-phase current is higher than C-phase current.

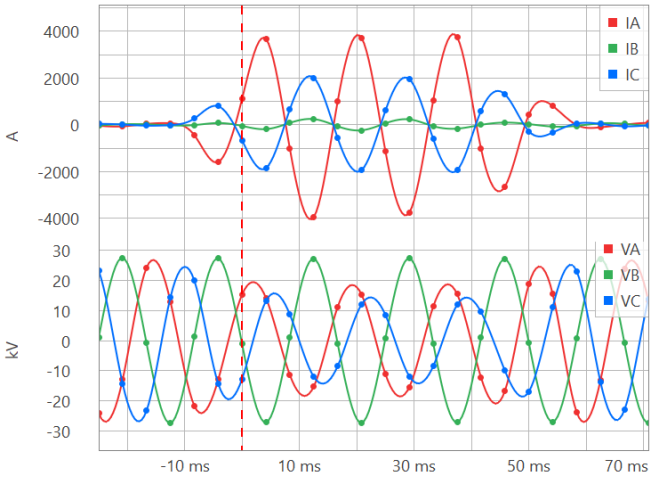

Fig. 5. Filtered voltages and currents of the Breaker 3 relays during the fault.

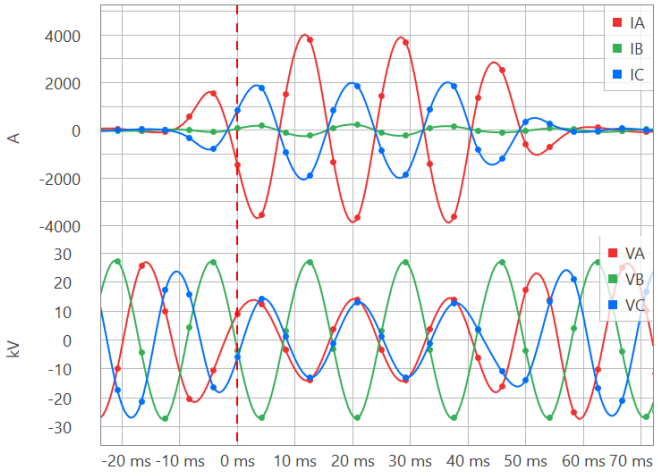

Fig. 6. Filtered voltages and currents of the Breaker 4 primary relay during the fault.

These current and voltage signatures are uncommon on the power system. The A-phase open series fault, in conjunction with the C-A shunt fault, provided a significant amount of zero-sequence current, as is shown in Fig. 7 and Fig. 8. This resulted in the Breaker 3 primary protective relay enabling its ground elements. Based on the currents and voltages identified by the Breaker 3 primary relay, the apparent impedance fell within the coverage of the Zone 1 quadrilateral element and led to an operation of the breaker. The Breaker 3 backup relay experienced the same amount of ground current as the primary relay, as is shown in Fig. 8.

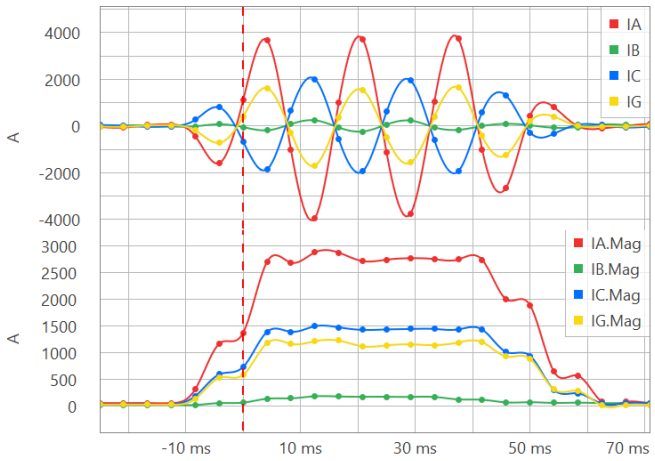

Fig. 7. Phase and residual filtered current measured by the Breaker 3 primary protective relay.

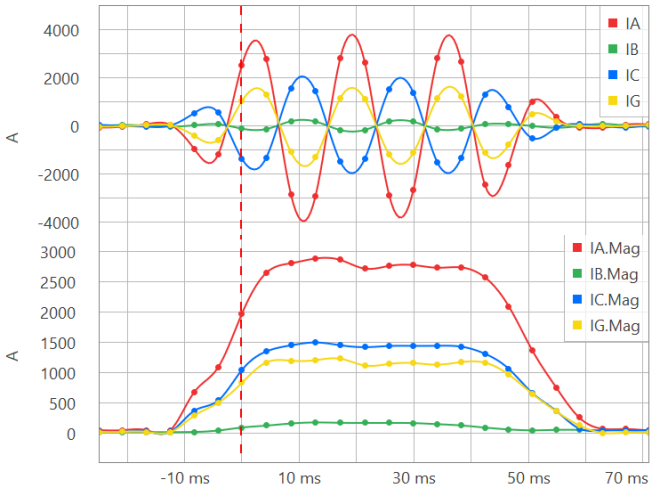

Fig. 8. Phase and residual filtered current measured by the Breaker 3 backup protective relay.

The natural question the utility asked the relay manufacturer is why the primary relay operated while the backup relay restrained. It is common for utilities to use different relay models for primary and backup protective relaying. The backup protective relay is a different model than the primary relay. The backup relay interpreted this fault as a phase-to-phase fault and did not enable its ground distance elements. Whereas the primary relay interpreted this fault as a ground fault and enabled its ground elements.

The unintended operation and the different decision between the primary and backup relay are what led the utility to reach out to the relay manufacturer, and together they investigated why the Breaker 3 primary relay operated.

There were two initial clues that helped the manufacturer and the utility discover the unknown open phase just outside Substation A. The first clue was that there was no A-phase current present through Breaker 1 during the fault. The second clue was that the voltage on A-phase did not depress more than C-phase when the current on A-phase was higher than C-phase. To get to root cause, these two clues were further investigated.

Since A-phase current on Breaker 1 was not present during the fault, it was helpful to investigate if it was present before the fault. Fig. 9 is a plot of current cycles before the trigger time in Fig. 3. Notice that A-phase pre-fault current is flat with a magnitude reflecting noise. In contrast, Fig. 10 shows that A-phase pre-fault current was passing through the other end of the line at Breaker 2. This led the investigators to think perhaps the current transformer (CT) was not providing information to the Breaker 1 protective relays. Field personnel were asked to confirm the state of the CTs to ensure no shorting existed.

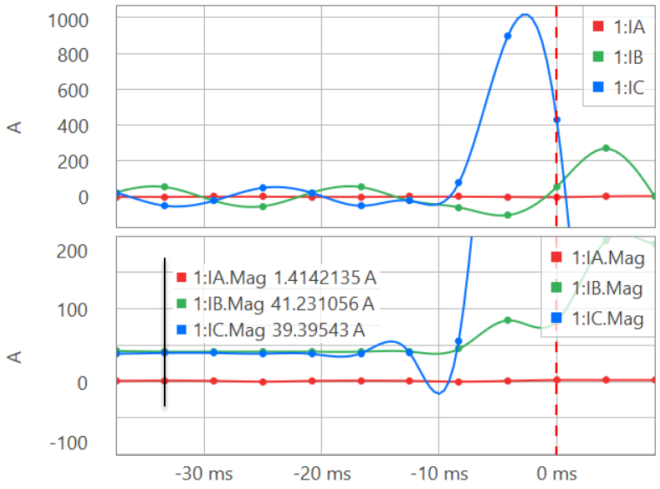

Fig. 9. Breaker 1 pre-fault current waveforms and magnitudes.

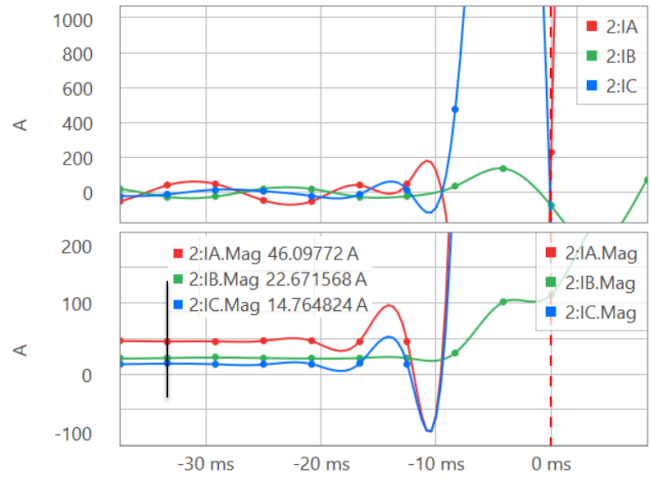

Fig. 10. Breaker 2 pre-fault current waveforms and magnitudes.

So, the investigators began to consider the other main clue: A-phase voltage was not depressing more than C-phase. They speculated that from the perspective of Breaker 3 protection the fault appeared to have ground involved. From the perspective of the Breaker 2 relays, the fault appeared to be more like a phase-to-phase fault. The investigators decided to plot the zero-sequence voltage measured at Substation A and Substation B to determine if the fault was phase-to-phase or phase-to-phase-ground. It is important to recall that the presence of zero-sequence voltage indicates that a ground fault is present. It is also important to recall that for a phase-to-phase-to-ground fault all sequence voltages are equal at the point of the fault [1]. As is shown in Table I , the zero-sequence voltage was very low compared to positive- and negative-sequence quantities. This led the investigators to strongly believe this was additional evidence that ground was not involved in the fault.

TABLE I
SUBSTATION A AND SUBSTATION B SEQUENCE VOLTAGES DURING THE FAULT

Substation A Sequence Voltages	V0	0.43∡30.62° kV
	V1	13.66∡0° kV
	V2	5.76∡6.41° kV
Substation B Sequence Voltages	V0	0.20∡–149.38° kV
	V1	10.51∡5.84° kV
	V2	8.60∡2.9° kV

The investigators came back to the question of why, for a phase-to-phase fault, is the A-phase current at Substation B so much higher than C-phase? But then why is the voltage being supported more on A-phase than C-phase? These two questions, coupled with the clue that current was not flowing through the Breaker 1 relays, spurred the investigators to hypothesize whether an open phase had occurred on the primary of the system instead of the CTs being shorted.

The investigators began to think how they might prove this hypothesis. They considered what the pre-fault voltages and currents looked like on both ends of Line 1. Fig. 11 shows the phase voltage and current phasors in the primary relays on both ends of the line.

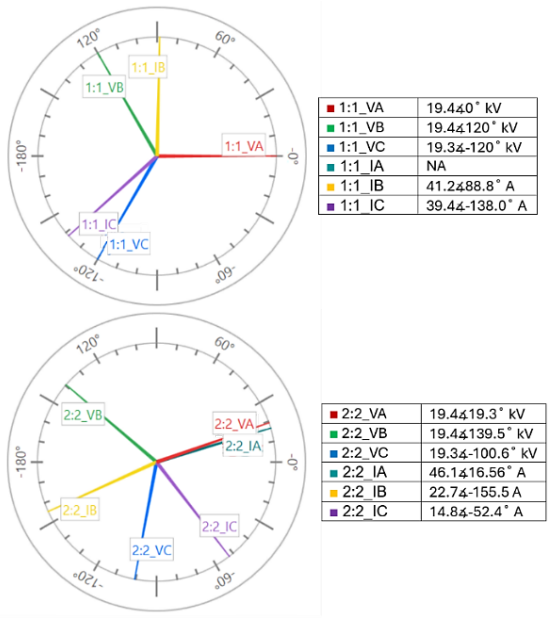

Fig. 11. Phasor diagrams of voltage and current. Breaker 1 quantities on the top and Breaker 2 quantities on the bottom.

First, it is important to notice the A-phase voltages and currents. At Substation A, A-phase current is nonexistent. At Substation B, A-phase current slightly lags A-phase voltage. Now observe the voltage and current angle relationship on B- and C-phases. The voltage angle at Substation B is leading the voltage angle at Substation A. Power is being delivered from Substation B to Substation A on B- and C-phases. For a balanced three-phase power system, a similar angle relationship between voltage and current would be expected for A-phase. But the power angle reflects a near unity power factor for A-phase. It is important to remember that in Fig. 2, there is load on the Substation B side of the open phase. Power flow through A-phase at Substation B was solely supporting load unlike B- and C-phases, which were supporting load and power transfer. This strengthened the hypothesis of an open phase.

Being armed with this knowledge, the uncharacteristic voltage and current waveforms, and the unlikelihood of two sets of CTs being shorted or opened, the hypothesis that this was indeed an open-phase condition was believed. The utility then initiated a meter command. Table II shows the result of that command, which included the local current of Breaker 2, the remote current of Breaker 1, and the vector sum of each quantity. Notice that almost 44 amperes are flowing through Substation B to the load on A-phase while nothing but noise is observed through Substation A. On B- and C-phases, it is important to observe that the difference of current between the two ends of the line is 43 amperes, which matches A-phase from Substation B feeding the tapped load. The remainder of current supports power transfer across the line. These data show that current was still not flowing through A-phase at Substation A. Based on this fact, a maintenance crew was dispatched to ride the line. They discovered a missing jumper nine spans outside of Substation A, which they replaced.

TABLE II
BREAKER 1 AND BREAKER 2 PRIMARY METERING QUANTITIES WITH VECTOR SUM

2	IA	43.74∡–6.9° A	I1	8.48∡0.0° A
	IB	13.09∡–105.4° A	3I0	41.6∡–11.3° A
	IC	9.7∡85.1° A	3I2	64.5∡7.2° A
1	IA	0.66∡–75.7° A	I1	34.96∡–9.4° A
	IB	54.05∡103.5° A	3I0	39.9∡168.6° A
	IC	51.51∡–121.2° A	3I2	65.4∡174.7° A
Vector sum	IA	43.98∡–7.6° A	I1	43.35∡–7.5° A
	IB	43.06∡111.9° A	3I0	1.7∡–8.9° A
	IC	43.02∡–126.9° A	3I2	2.3∡–118.9° A

III. OPEN-PHASE CONDITION DETECTION METHODS

The missing jumper on A-phase created an open-phase condition on Line 1. How long the jumper had been missing is unknown. If the open phase could have been detected and corrected before the phase-to-phase fault occurred, a simultaneous fault would not have happened. The following section describes methods for detecting an open-phase condition.

The most straightforward method is to set either a residual or negative-sequence overcurrent element with a low pickup and a significant time delay and set it solely for alarming purposes. Current unbalance is low on transmission and subtransmission lines. As a general rule, the current unbalance expected on transmission and subtransmission lines is less than 10 percent of nominal current on a line. When unbalance drastically increases, it is due to either a shunt or series fault. If unbalance lasts for a significant amount of time, it could be indicative of a problem and monitored through an alarm to a

supervisory control and data acquisition (SCADA) system. It is evident in Table II that both the Breaker 1 and Breaker 2 residual and negative-sequence current quantities are much higher than expected, compared to the amount of positive-sequence current. The challenge with this method is to set a threshold that is high enough during peak load where nuisance alarms due to natural unbalance do not occur but low enough during low load to detect an open phase.

The next method would be to set an instantaneous overcurrent element that is comparing individual phase current to a low set threshold. For the greatest sensitivity, the minimum overcurrent pickup setting allowable could be selected. Then the method would evaluate if there is a discrepancy between one phase and the other two. If one phase is below the threshold but the other two are not, this is an unusual condition and should be monitored through an alarm to a SCADA system. If all three phases are above or below the threshold, nothing is done. Fig. 12 is a logic diagram of this solution. Multiple tapped lines or low current challenges the detection aspect of this method.

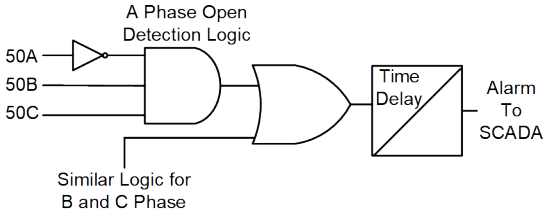

Fig. 12. Open-phase detection logic using overcurrent comparisons.

Another method that is available in more advanced microprocessor relays is a comparison of the ratio of the negative-sequence current to the positive-sequence current. Since current unbalance is low on transmission and subtransmission lines, negative-sequence current is low and positive-sequence current is high. In normal conditions, the negative-sequence to positive-sequence ratio will be low. When an open-phase condition occurs, negative-sequence current increases even with multiple tapped loads present. This will increase the negative-sequence to positive-sequence ratio. This ratio can then be compared to a percentage ratio threshold to evaluate if there is an unusual system configuration. To determine this percentage ratio threshold, Roberts and Guzmán [2] simulate a three-phase fault assuming no source impedance and with the remote terminal(s) open to evaluate how much negative-sequence to positive-sequence current there is. If the percentage ratio threshold is above this value, a negative-sequence directional element will remain secure during three-phase faults. If an open-phase condition occurs, the ratio of negative-sequence to positive-sequence current will likely cross the percentage ratio threshold. Then, it is necessary to monitor this condition for a set time delay and then alarm to SCADA. This logic should be supervised by a load current detector to prevent spurious alarms that may occur during light load and also be supervised by a condition that monitors if a fault is occurring or not.

Breaker 1 protective relays could have implemented either the first or last open-phase detection method. The protective relays implemented have a negative-sequence voltage-polarized element. This element is enabled by three checks: the negative-sequence to positive-sequence ratio is above a certain threshold, which by default is set to ten percent; the negative-sequence current is above a minimum threshold, which by default is set to a quarter of an ampere; and none of the poles of the breaker are open. If all three of these conditions are true, word bit 32QE asserts. Even though this word bit is used to enable the negative-sequence voltage-polarized element, it may be used for open-phase detection as well. Fig. 13 is the logic diagram that could implement this open-phase detection method in this relay by incorporating the light loading and fault monitoring checks previously mentioned. Fig. 14 shows that the negative-sequence to positive-sequence ratio was above the ratio threshold and that the 32QE word bit was asserted before the phase-to-phase fault occurred, which initiated at the red dashed line.

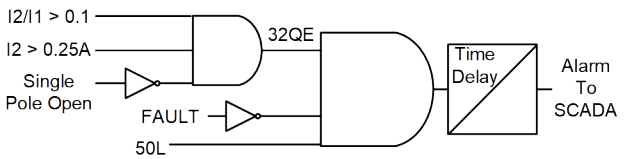

Fig. 13. Open-phase detection method using negative-sequence to positive-sequence ratio comparison.

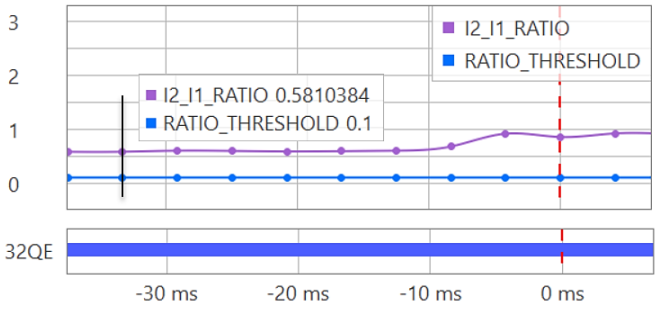

Fig. 14. Negative-sequence to positive-sequence ratio threshold word bit asserted.

The last method to mention is available in the most advanced microprocessor relays. This method detects open-phase conditions along with falling broken conductors by evaluating changes to the local terminal current immediately after the broken conductor or open-phase condition occurs. Reference [3] presents this method and its advantages in detail.

IV. Brief Overview of Symmetrical Components and Phase Components

So far, the analysis performed has been troubleshooting based on empirical data after the simultaneous fault occurred. However, circuit analysis can be used to gain further insight into the faulted circuit and the currents and voltages observed at the time of the fault. The following sections explore this aspect of the fault analysis.

In the early to mid-1900s, the advent of symmetrical components gave engineers a new way to analyze and understand faulted power systems. Of particular interest to protection engineers is solving for unknown quantities, such as fault current in a power system circuit, where the fault type, fault location, and fault impedance are all variable.

Symmetrical components allow for the transformation of magnetically coupled three-phase power system circuits into three separate uncoupled networks called sequence networks. The three sequence networks are referred to as positive, negative, and zero. The sequence networks for a particular system can be drawn out and connected in different configurations based on the fault type being analyzed. The connected sequence network circuit can then be analyzed using Thevenin's theorem and Ohm's law to solve for the currents through each of the sequence networks. Once these sequence currents are solved for, they can then be used to obtain the phase-domain currents. There are many thorough sources that discuss the theory and procedures for solving circuits with a single fault using symmetrical components [1] [4].

Using symmetrical components to solve power systems with a simultaneous fault condition is a more involved process, which also requires different circuit analysis techniques. Two fundamental sources for analyzing simultaneous faults using this method are [1] and [5]. The procedure involves using Z-bus impedance matrices to develop two-port sequence networks, which are then connected based on the fault type. A quick glance at the connected two-port network circuits, and the analysis involved in solving these may seem daunting and unfamiliar due to the differences from solving for single faults using the traditional method.

Prior to the advent of symmetrical components, in the mid-1800s, Kirchhoff's laws could be used to write a system of simultaneous equations to solve for unknown quantities in a circuit. The difficulty of this method is that a simple radial power system circuit with an unbalanced fault resolves to a system of three simultaneous equations with complex numbers. More complex faulted circuits, like looped systems or parallel line systems, will resolve into larger systems of simultaneous equations. Solving systems that consist of any more than three simultaneous equations becomes an arduous or impossible task if using traditional paper and pencil linear algebra. However, with modern computing tools we are not limited in the same way as engineers in the early 1900s. A computer program can carry the burden of the linear algebra, which makes phase-domain analysis a viable option.

A benefit of solving faulted power system circuits in the phase domain is that for all fault types it is only necessary to solve for a single-circuit topology. For this single-circuit model, the fault location, fault impedance, and fault type are variables that can be easily adjusted within the computer program. However, solving power system circuits in the phase domain does require modeling mutual coupling, which may not be feasible if solving these circuits by hand. In contrast, if using the sequence component and two-port network method, changing the fault type requires solving for a new circuit topology, but it does provide the benefit of decoupling, which can be advantageous for paper and pencil analysis.

Phase-domain circuit analysis requires Kirchhoff's voltage law (KVL) equations to be written and used for the circuit model. This process for circuit analysis is likely familiar for most electrical engineers but does require some bookkeeping mathematics, which will be covered in Section V.

V. Phase Component Analysis of a Parallel Line

The following section will demonstrate the process of phase component analysis of a parallel line with a single fault and with a simultaneous fault condition. The parallel line circuit model presented in this paper is only an approximation of the power system in this case study. The goal is to provide a simple first-principles analysis technique for troubleshooting and insight into nontextbook fault cases. The parallel line system derived in [6] will be used as a basis, however, the circuit model requires some customization. The procedure and mathematics for this customization will be illustrated to demonstrate the flexibility of the parallel line circuit model and how this might be applied for different simultaneous fault types. The line and source impedance values are derived from the positive-sequence and zero-sequence line impedance and source impedance values provided by the utility. We use the following transformations to obtain the corresponding self and mutual impedances for the circuit model [7].

$$Z_S = \frac{1}{3}(Z_0 + 2Z_1)$$

$$Z_M = \frac{1}{3}(Z_0 - Z_1)$$

The circuit model requires separate line self-impedances for each phase. This will allow modeling the series fault where the A-phase line between Breakers 1 and 2 in Fig. 1 is open. In Fig. 15, this is shown as $Z_{SA\ L1\ B1}$. We accomplish this by adjusting the A-phase line self-impedance variable at Breaker 1 to a number many orders of magnitude greater than other impedance values in the circuit. With separate self and mutual impedance terms, we are also able to account for a slight difference in the line impedance values for Lines 1 and 2. For simplicity, we do not model the tapped load between Breakers 1 and 2 and we keep the source voltage angles the same for a no-load condition. Finally, we remove the term for the mutual impedance between Lines 1 and 2, as this is negligible due to the topology of this particular circuit.

The three-phase circuit used for the analysis is shown in Fig. 15. KVL is used to develop the nine simultaneous equations for the circuit. We follow the procedure in [6] for developing the nine simultaneous equations while also accounting for the necessary modifications to the general circuit model. The goal is to solve for the unknown currents I_{AS}, I_{BS}, I_{CS}, I_{AR}, I_{BR}, I_{CR}, I_{AP}, I_{BP}, and I_{CP}.

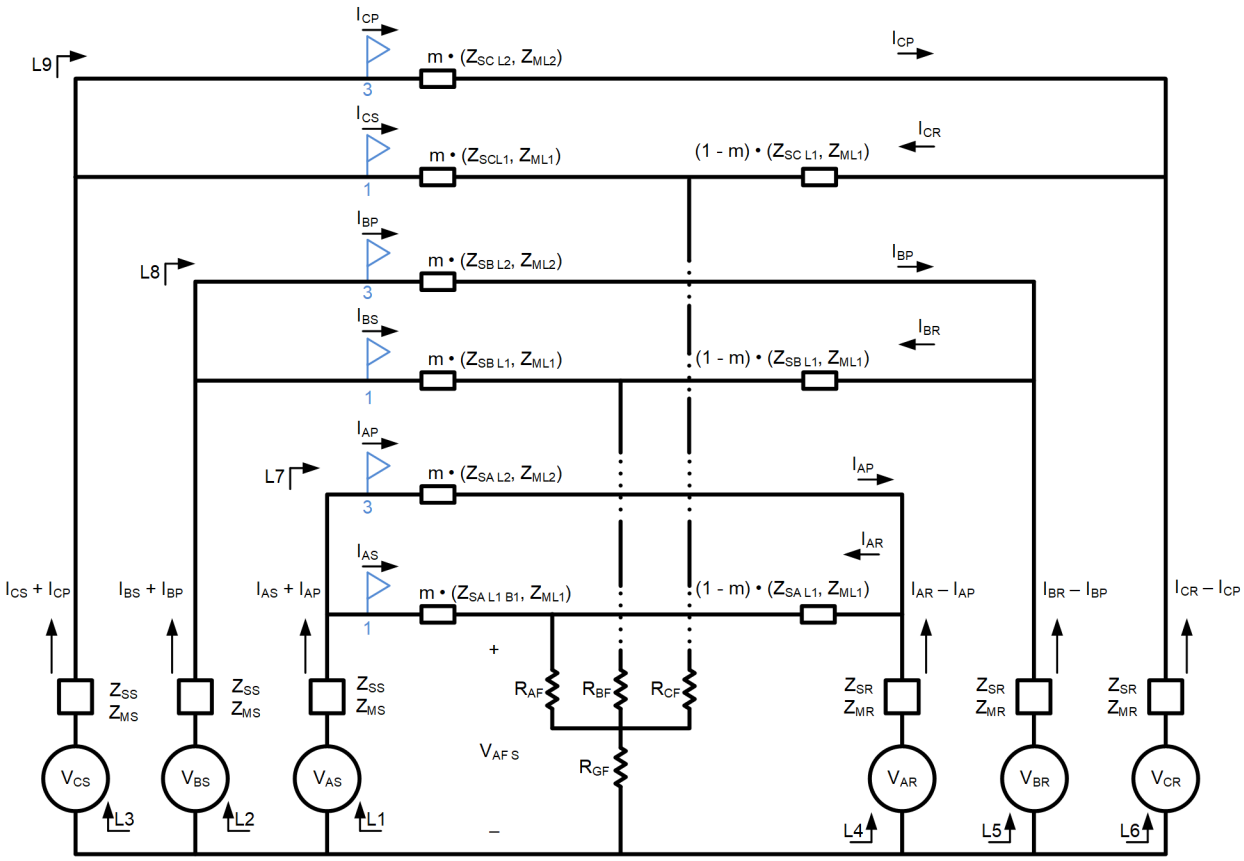

Fig. 15. Three-phase circuit model.

A. *Procedure for Equations 1, 2,and 3*

We begin with writing a KVL equation relative to L1, which will start at the S-side voltage source V_{AS} and will end at the fault voltage V_{AF_S}, in which V_{AF_S} is the voltage drop across the fault impedance R_{AF} and R_{GF}. Solve this equation for V_{AF_S}.

$$\begin{aligned} V_{AF\,S} = {} & V_{AS} - (I_{AS} + I_{AP}) \bullet Z_{SS} \\ & -(I_{BS} + I_{BP} + I_{CS} + I_{CP}) \bullet Z_{MS} \\ & - I_{AS} \bullet m \bullet Z_{SA\,L1\,B1} \\ & -(I_{BS} + I_{CS}) \bullet m \bullet Z_{ML1} \end{aligned}$$

We then write a KVL equation relative to L4, which will start at the R-side voltage source V_{AR} and will end at the fault voltages V_{AF_R}, in which V_{AF_R} is the voltage drop across the fault impedance R_{AF} and R_{GF}. The following equation will solve for V_{AF_R}.

$$\begin{aligned} V_{AF\,R} = {} & V_{AR} - (I_{AR} - I_{AP}) \bullet Z_{SR} \\ & -(I_{BR} - I_{BP} + I_{CR} - I_{CP}) \bullet Z_{MR} \\ & - I_{AR} \bullet (1 - m) \bullet Z_{SA\,L1} \\ & -(I_{BR} + I_{CR}) \bullet (1 - m) \bullet Z_{ML1} \end{aligned}$$

We know that $V_{AF\,S} = V_{AF\,R}$, which we further developed to $V_{AF\,S} - V_{AF\,R} = 0$. We then substitute in equations for $V_{AF\,S}$ and $V_{AF\,R}$. Finally, we solve for $V_{AS} - V_{AR}$, which will result with the first equation.

$$\begin{aligned} V_{AS} - V_{AR} = {} & I_{AS} \bullet (Z_{SS} + m \bullet Z_{SA\,L1\,B1}) \\ & + I_{BS} \bullet (Z_{MS} + m \bullet Z_{ML1}) \\ & + I_{CS} \bullet (Z_{MS} + m \bullet Z_{ML1}) \\ & + I_{AR} \bullet (-Z_{SR} - (1 - m) \bullet Z_{SA\,L1}) \\ & + I_{BR} \bullet (-Z_{MR} - (1 - m) \bullet Z_{ML1}) \\ & + I_{CR} \bullet (-Z_{MR} - (1 - m) \bullet Z_{ML1}) \\ & + I_{AP} \bullet (Z_{SS} + Z_{SR}) \\ & + I_{BP} \bullet (Z_{MS} + Z_{MR}) \\ & + I_{CP} \bullet (Z_{MS} + Z_{MR}) \end{aligned}$$

This process can be repeated for the B-phase and C-phase, which will give the second and third equations.

B. *Procedure for Equations 4, 5, and 6*

The procedure begins with writing a KVL equation relative to L1, which starts at the S-side voltage source V_{AS}, however, this time we include the R-side A-phase, B-phase, and C-phase currents through the appropriate fault resistances. The next step is to solve this equation for V_{AS}.

$$\begin{aligned} V_{AS} = {} & I_{AS} \bullet Z_{SS} \\ & + I_{AP} \bullet Z_{SS} \\ & +(I_{BS} + I_{BP} + I_{CS} + I_{CP}) \bullet Z_{MS} \\ & + I_{AS} \bullet m \bullet Z_{SA\,L1\,B1} \\ & +(I_{BS} + I_{CS}) \bullet m \bullet Z_{ML1} \\ & +(I_{AS} + I_{AR}) \bullet R_{AF} \\ & +(I_{AS} + I_{AR} + I_{BS} + I_{BR} + I_{CS} + I_{CR}) \bullet R_{GF} \end{aligned}$$

The solution for V_{AS} can be further refined by grouping terms, which results in the fourth equation.

$$\begin{aligned} V_{AS} = {} & I_{AS} \bullet (Z_{SS} + m \bullet Z_{SA\,L1\,B1} + R_{AF} + R_{GF}) \\ & + I_{BS} \bullet (Z_{MS} + m \bullet Z_{ML1} + R_{GF}) \\ & + I_{CS} \bullet (Z_{MS} + m \bullet Z_{ML1} + R_{GF}) \\ & + I_{AR} \bullet (R_{AF} + R_{GF}) + I_{BR} \bullet (R_{GF}) + I_{CR} \bullet (R_{GF}) \\ & + I_{AP} \bullet (Z_{SS}) + I_{BP} \bullet (Z_{MS}) + I_{CP} \bullet (Z_{MS}) \end{aligned}$$

The process for the B-phase and C-phase can be repeated, which will give the fifth and sixth equations.

C. *Procedure for Equations 7, 8, and 9*

The procedure begins with writing a KVL equation relative to L7, which will start at the S-side source V_{AS} and end at the voltage drop across the R-side source impedance. The voltage drop on the R side will be designated $V_{AR\,S}$ in this equation. The next step is to solve for $V_{AR\,S}$.

$$\begin{aligned} V_{AR\,S} = V_{AS} - (I_{AS} + I_{AP}) \bullet Z_{SS} \\ -(I_{BS} + I_{BP} + I_{CS} + I_{CP}) \bullet Z_{MS} \\ -I_{AP} \bullet Z_{SA\,L2} - (I_{BP} + I_{CP}) \bullet Z_{ML2} \end{aligned}$$

The next step is to write an equation that solves for the voltage drop on the R-side source, $V_{AR\,R}$.

$$\begin{aligned} V_{AR\,R} = V_{AR} - (I_{AR} - I_{AP}) \bullet Z_{SR} \\ -(I_{BR} - I_{BP} + I_{CR} - I_{CP}) \bullet Z_{MR} \end{aligned}$$

We know that $V_{AR\,S} = V_{AR\,R}$, which can be further developed so that $V_{AR\,S} - V_{AR\,R} = 0$. We then substitute in equations for $V_{AR\,S}$ and $V_{AR\,R}$. Finally, we solve for $V_{AS} - V_{AR}$, which will result inequation 7.

$$\begin{aligned} V_{AS} - V_{AR} = I_{AS} \bullet (Z_{SS}) + I_{BS} \bullet (Z_{MS}) + I_{CS} \bullet (Z_{MS}) \\ + I_{AR} \bullet (-Z_{SR}) \\ + I_{BR} \bullet (-Z_{MR}) \\ + I_{CR} \bullet (-Z_{MR}) \\ + I_{AP} \bullet (Z_{SS} + Z_{SA\,L2} + Z_{SR}) \\ + I_{BP} \bullet (Z_{MS} + Z_{ML2} + Z_{MR}) \\ + I_{CP} \bullet (Z_{MS} + Z_{ML2} + Z_{MR}) \end{aligned}$$

The process can be repeated for the B-phase and C-phase, which will give the eighth and ninth equations.

The nine equations are then organized into the following matrix format.

$$\begin{bmatrix} V_{AS} - V_{AR} \\ V_{BS} - V_{BR} \\ V_{CS} - V_{CR} \\ V_{AS} \\ V_{BS} \\ V_{CS} \\ V_{AS} - V_{AR} \\ V_{BS} - V_{BR} \\ V_{CS} - V_{CR} \end{bmatrix} = \begin{bmatrix} [UL]\ [UM]\ [UR] \\ [ML]\ [MM]\ [MR] \\ [BL]\ [BM]\ [BR] \end{bmatrix} \begin{bmatrix} I_{AS} \\ I_{BS} \\ I_{CS} \\ I_{AR} \\ I_{BR} \\ I_{CR} \\ I_{AP} \\ I_{BP} \\ I_{CP} \end{bmatrix}$$

$$[UL] = \begin{bmatrix} Z_{SS} + m \bullet Z_{SA\,L1\,B1} & Z_{MS} + m \bullet Z_{ML1} & Z_{MS} + m \bullet Z_{ML1} \\ Z_{MS} + m \bullet Z_{ML1} & Z_{SS} + m \bullet Z_{SB\,L1} & Z_{MS} + m \bullet Z_{ML1} \\ Z_{MS} + m \bullet Z_{ML1} & Z_{MS} + m \bullet Z_{ML1} & Z_{SS} + m \bullet Z_{SC\,L1} \end{bmatrix}$$

$$[UM] = \begin{bmatrix} -Z_{SR} - (1-m) \bullet Z_{SA\,L1} & -Z_{MR} - (1-m) \bullet Z_{ML1} & -Z_{MR} - (1-m) \bullet Z_{ML1} \\ -Z_{MR} - (1-m) \bullet Z_{ML1} & -Z_{SR} - (1-m) \bullet Z_{SB\,L1} & -Z_{MR} - (1-m) \bullet Z_{ML1} \\ -Z_{MR} - (1-m) \bullet Z_{ML1} & -Z_{MR} - (1-m) \bullet Z_{ML1} & -Z_{SR} - (1-m) \bullet Z_{SC\,L1} \end{bmatrix}$$

$$[UR] = \begin{bmatrix} Z_{SS} + Z_{SR} & Z_{MS} + Z_{MR} & Z_{MS} + Z_{MR} \\ Z_{MS} + Z_{MR} & Z_{SS} + Z_{SR} & Z_{MS} + Z_{MR} \\ Z_{MS} + Z_{MR} & Z_{MS} + Z_{MR} & Z_{SS} + Z_{SR} \end{bmatrix}$$

$$[ML] = \begin{bmatrix} Z_{SS} + m \bullet Z_{SA\,L1\,B1} + R_{AF} + R_{GF} & Z_{MS} + m \bullet Z_{ML1} + R_{GF} & Z_{MS} + m \bullet Z_{ML1} + R_{GF} \\ Z_{MS} + m \bullet Z_{ML1} + R_{GF} & Z_{SS} + m \bullet Z_{SB\,L1} + R_{BF} + R_{GF} & Z_{MS} + m \bullet Z_{ML1} + R_{GF} \\ Z_{MS} + m \bullet Z_{ML1} + R_{GF} & Z_{MS} + m \bullet Z_{ML1} + R_{GF} & Z_{SS} + m \bullet Z_{SC\,L1} + R_{CF} + R_{GF} \end{bmatrix}$$

$$[MM] = \begin{bmatrix} R_{AF} + R_{GF} & R_{GF} & R_{GF} \\ R_{GF} & R_{BF} + R_{GF} & R_{GF} \\ R_{GF} & R_{GF} & R_{CF} + R_{GF} \end{bmatrix}$$

$$[MR] = \begin{bmatrix} Z_{SS} & Z_{MS} & Z_{MS} \\ Z_{MS} & Z_{SS} & Z_{MS} \\ Z_{MS} & Z_{MS} & Z_{SS} \end{bmatrix}$$

$$[BL] = \begin{bmatrix} Z_{SS} & Z_{MS} & Z_{MS} \\ Z_{MS} & Z_{SS} & Z_{MS} \\ Z_{MS} & Z_{MS} & Z_{SS} \end{bmatrix}$$

$$[BM] = \begin{bmatrix} -Z_{SR} & -Z_{MR} & -Z_{MR} \\ -Z_{MR} & -Z_{SR} & -Z_{MR} \\ -Z_{MR} & -Z_{MR} & -Z_{SR} \end{bmatrix}$$

$$[BR] = \begin{bmatrix} Z_{SS} + Z_{SA\,L2} + Z_{SR} & Z_{MS} + Z_{ML2} + Z_{MR} & Z_{MS} + Z_{ML2} + Z_{MR} \\ Z_{MS} + Z_{ML2} + Z_{MR} & Z_{SS} + Z_{SB\,L2} + Z_{SR} & Z_{MS} + Z_{ML2} + Z_{MR} \\ Z_{MS} + Z_{ML2} + Z_{MR} & Z_{MS} + Z_{ML2} + Z_{MR} & Z_{SS} + Z_{SC\,L2} + Z_{SR} \end{bmatrix}$$

The general matrix equation is then rearranged to solve for the current matrix. It is at this point that a computer program can be used to perform the linear algebra, effectively giving users a simulation of the circuit model.

$$[\text{Current}] = [\text{Impedance}]^{-1}[\text{Voltage}]$$

Once the unknown current values are solved for, solving for the voltages at the Breaker 3 relay location simply involves taking the S-side source voltage and subtracting the voltage drop across the source impedances.

$$V_{A\,B1} = V_{AS} - Z_{SS} \bullet (I_{AS} + I_{AP}) - Z_{MS} \bullet (I_{BS} + I_{BP} + I_{CS} + I_{CP})$$
$$V_{B\,B1} = V_{BS} - Z_{SS} \bullet (I_{BS} + I_{BP}) - Z_{MS} \bullet (I_{AS} + I_{AP} + I_{CS} + I_{CP})$$
$$V_{C\,B1} = V_{CS} - Z_{SS} \bullet (I_{CS} + I_{CP}) - Z_{MS} \bullet (I_{AS} + I_{AP} + I_{BS} + I_{BP})$$

VI. Phase-Domain Circuit Analysis Results

Initially, the simultaneous fault in the case study was believed to only involve a single C-A phase fault. After closer inspection, it was determined that the voltage and current phasors, while similar, were not characteristic of a true C-A phase fault. For a C-A phase fault on a homogonous system, we expect the C-phase and A-phase currents to be equal in magnitude and perfectly out of phase, while the C-phase and A-phase voltages are depressed in magnitude and the angle between them is reduced. Based on these boundary condition relationships, we can infer that the sequence quantities present for the phase-to-phase fault will be the positive and negative sequences and that the sequence networks will be connected in parallel, such that I1 and I2 will be equal in magnitude and perfectly out of phase [1][4].

The parallel line circuit model simulation can be used to show the expected voltage and current phasors at the relay location for Breaker 3, which would be present if we only consider the C-A shunt fault shown in Fig. 1. We can also derive the sequence currents and compare them to the expected outcome for a single C-A shunt fault condition. To achieve this, we set the fault impedances for the C-phase and A-phase to zero, while setting the B-phase and ground fault impedances to a number many orders of magnitude greater than the fixed circuit impedance values. Fig. 16 shows the results of the simulation.

The simulation results show the C-phase and A-phase currents are equal in magnitude and approximately 180 degrees out of phase while the voltage magnitudes are depressed and the angle between them has been reduced. We also observe that the zero-sequence current I0 is 0 amperes, and that the phase-to-phase fault only contains positive- and negative-sequence currents I1 and I2. The magnitudes of I1 and I2 are equal, and they are out of phase with each other. This is the expected result for a C-A phase fault. Based on the results, and the investigators prior experience with phase-to-phase shunt faults, the event report data presented in the case study did not line up with the expected current and voltage phasor relationships.

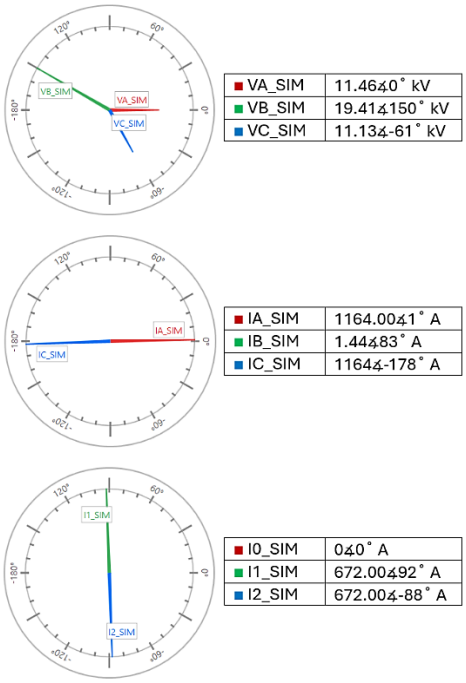

Fig. 16. Voltage and current phasors at Breaker 3 relay for C-A phase fault.

We now use the phase-domain simulation to show the phase voltages, phase currents, and sequence currents with only the A-phase series fault applied. To achieve this, we remove the C-A shunt fault by adjusting all shunt fault impedance values to be many orders of magnitude greater than the fixed circuit impedances. We also adjust the line self-impedance value associated with the A-phase at Breaker 1 to be many orders of magnitude greater than the fixed circuit impedances. Fig. 17 shows the result of this series fault simulation.

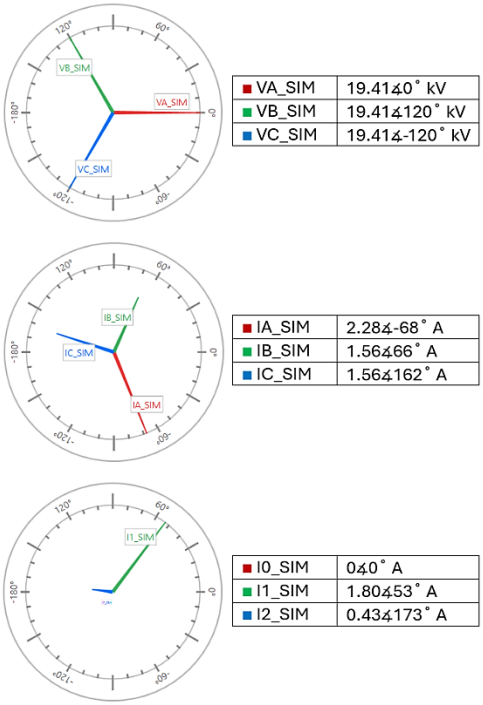

Fig. 17. Voltage and current phasors at Breaker 3 relay for A-phase series fault associated with Breaker 1 on Line 1.

The A-phase series fault results in the A-phase current at Breaker 3 being significantly larger in magnitude compared to the B-phase and C-phase currents, while the phase voltages are unaffected by the series fault.

Finally, we apply the simultaneous fault condition to the phase-domain circuit simulation. To achieve this, we combine the parameters for the C-A shunt fault and A-phase series faults analyzed previously. Notice that for the three different fault scenarios (C-A phase fault, A-phase series fault, and simultaneous fault) that only the single-circuit topology shown in Fig. 15 was used, and that for each fault scenario we simply adjust the corresponding impedance values. Fig. 18 compares the field event report data and the phase-domain circuit results at the time of the Zone 1 ground distance element operation.

For the simultaneous fault condition, the simulation and field event data show that the C-phase and A-phase currents are 177 degrees out of phase. We also observe the A-phase current magnitude is significantly greater than the C-phase. Despite this relationship in the current magnitudes, we see the A-phase voltage is less depressed in magnitude than the C-phase voltage.

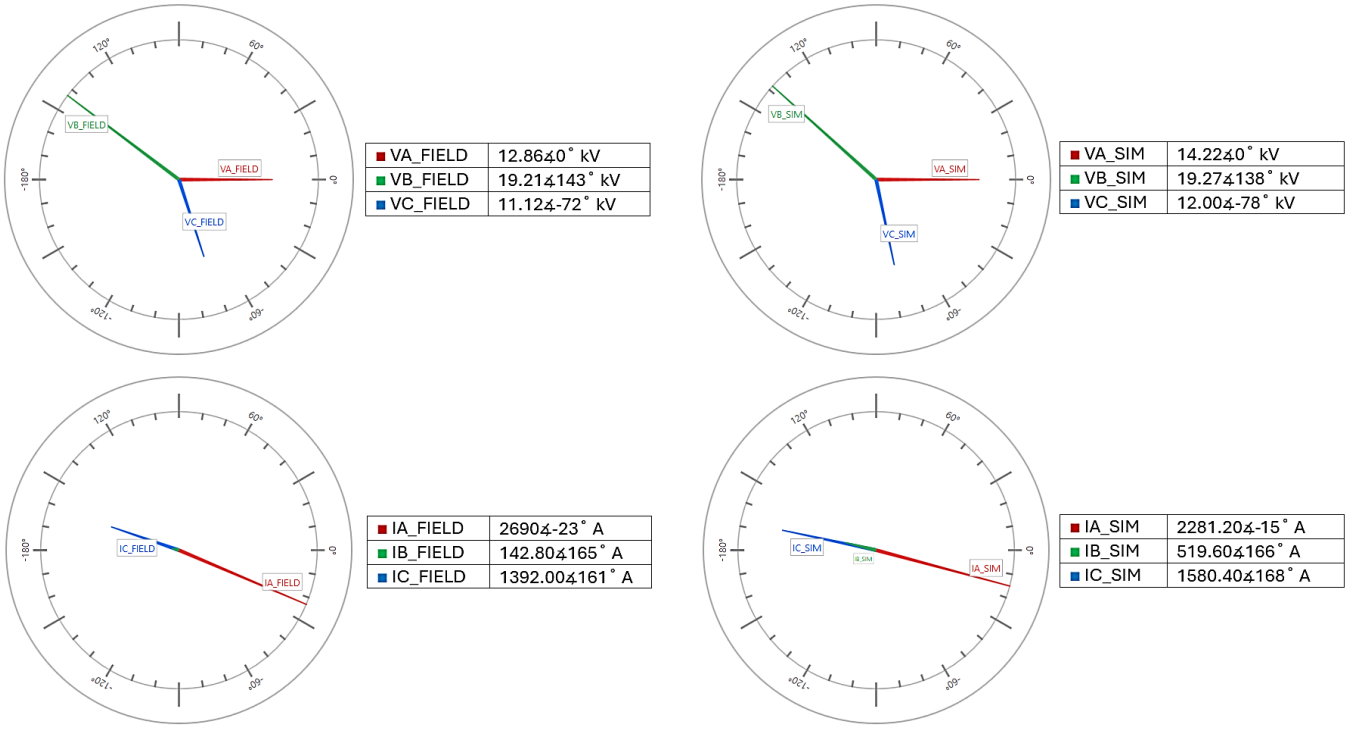

Fig. 18. Comparison of voltage and current phasors at Breaker 3 relay for simultaneous fault.

The results of the phase-domain simulation are closely comparable to the field event report data. The phase-domain solution makes some assumptions that are important to consider. Even though the phase-domain model is capable of modeling load flow, we omitted this detail from the solution presented here for the sake of simplicity. Also, the utility provided Thevenin-equivalent positive- and zero-sequence impedance values of the system impedances behind the bus. These values were used to model the source impedances, which may be less deterministic than using the line impedance values to model the lines. However, despite these assumptions, we see a good correlation between the field event data and the simulation data, not just for the relay at Breaker 3, but also for the relays at Breakers 1, 2, and 4, as can be observed in Fig. 19, Fig. 20, and Fig. 21.

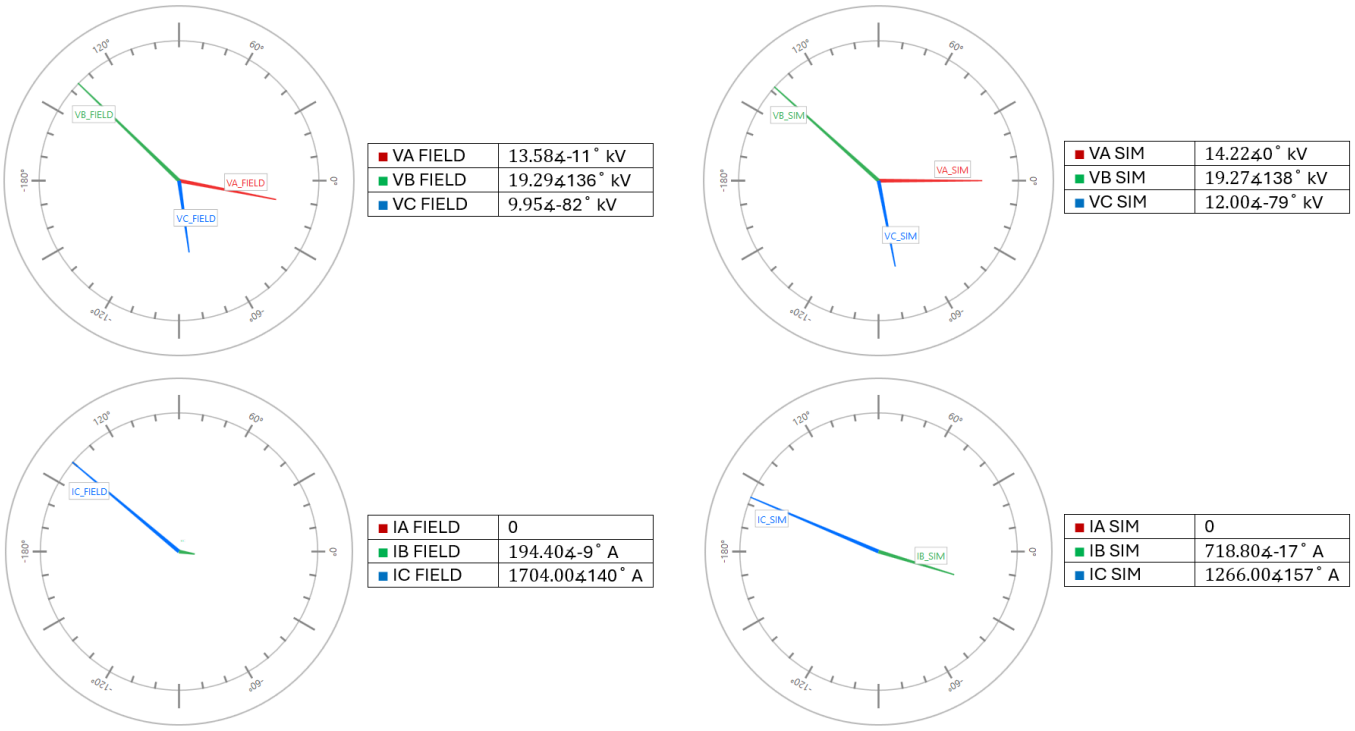

Fig. 19. Comparison of voltage and current phasors at Breaker 1 relay for simultaneous fault.

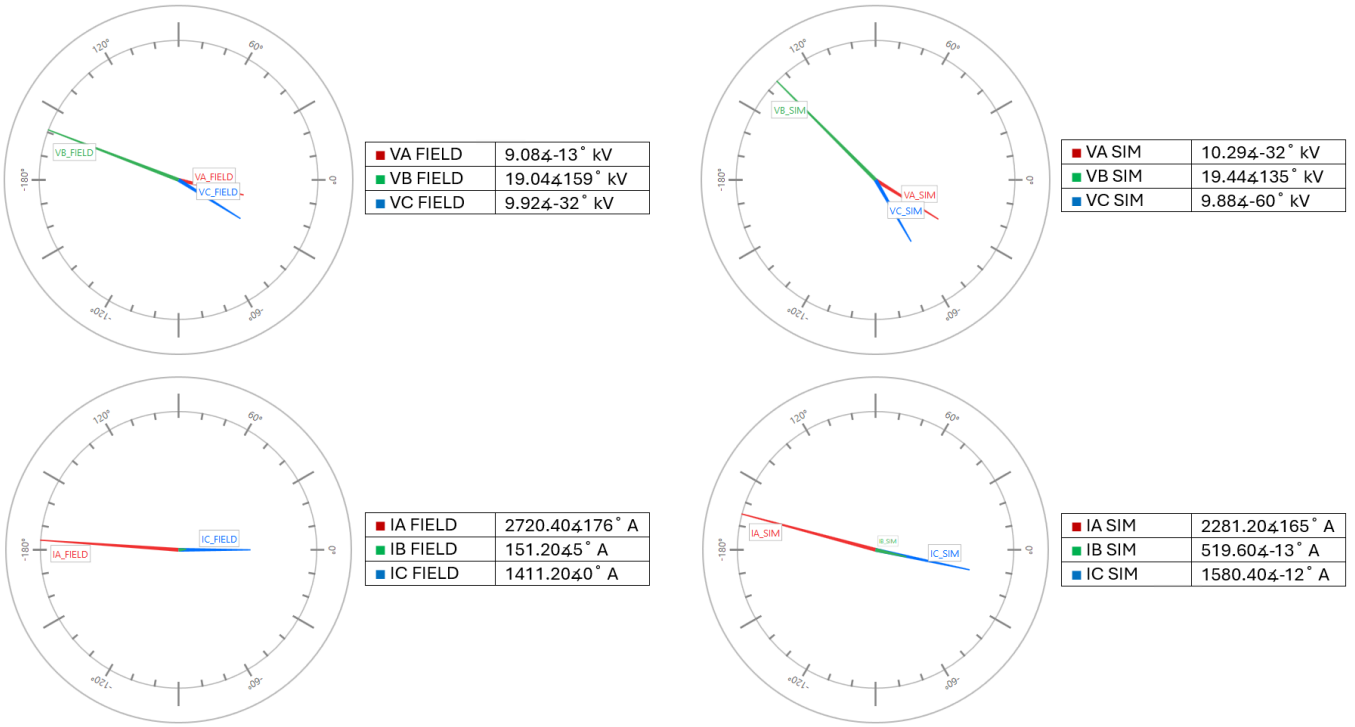

Fig. 20. Comparison of voltage and current phasors at Breaker 4 relay for simultaneous fault.

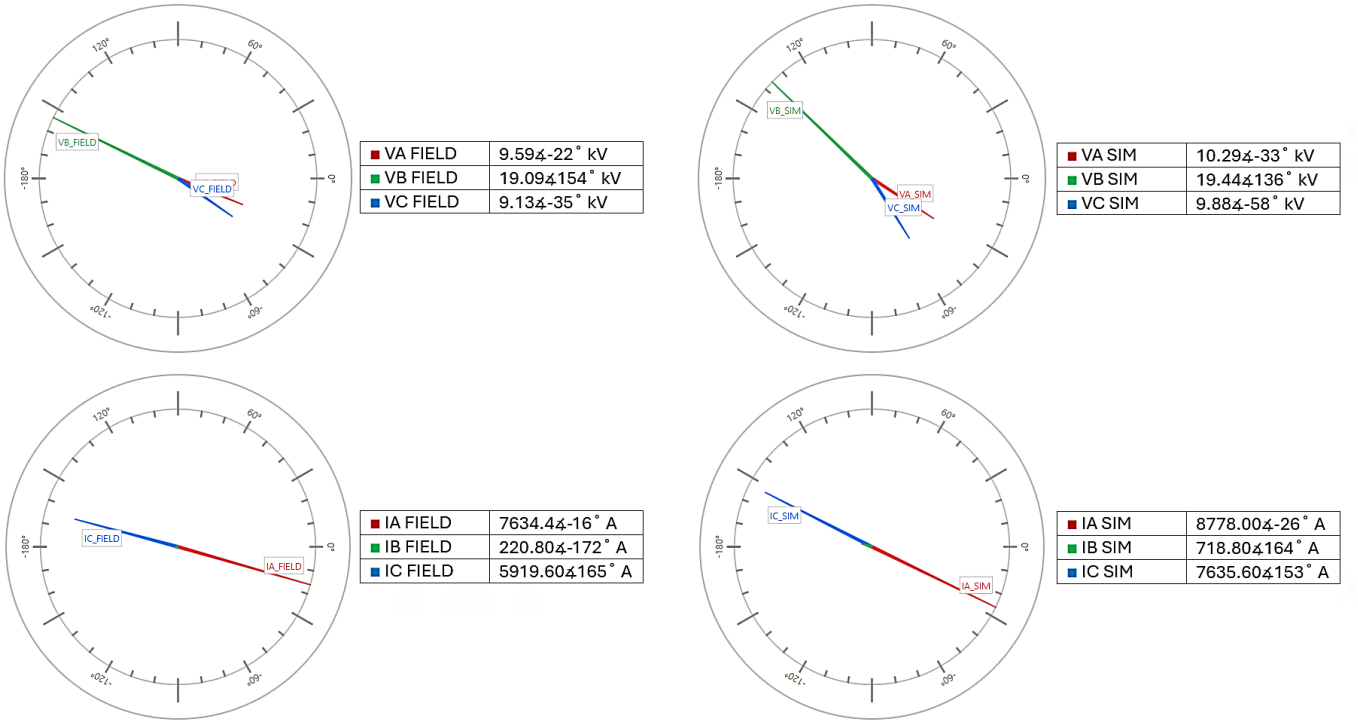

Fig. 21. Comparison of voltage and current phasors at Breaker 2 relay for simultaneous fault.

The benefit of this analysis is that while we can easily identify a C-A phase fault in an event report, it may not be as intuitive to identify and conceptualize the fault voltages and currents for a simultaneous fault like the one presented in this case study. Even after discovering that the A-phase series fault was present, and that it was most likely the contributing factor that challenged the Zone 1 distance element protection, it may be necessary or desirable to further analyze the power system circuit to be sure that root cause has been determined. The phase-domain circuit simulation is a first-principles approach that aids in event analysis for nontextbook faults.

VII. Conclusion

While rare in most cases, simultaneous faults can occur due to persistent preexisting conditions like an open phase, otherwise known as a series fault. In a scenario like this, Murphy's Law tells us that it is only a matter of time until a shunt fault occurs in conjunction with the standing series fault, and, thus, a simultaneous fault will occur. Series faults can be nondestructive compared to shunt faults and may go undetected. However, as shown in the case study, it is desirable to detect and account for these faults. Load detection elements or elements that compare positive- and negative-sequence current can be employed to notify system operators of open-phase conditions. These preventative measures can help mitigate the possibility that a series fault and a shunt fault occur at the same time. Simultaneous faults can challenge distance protection, which then necessitates in-depth event analysis to determine root cause. The event analysis and troubleshooting process for simultaneous fault conditions can be challenging due to the presence of nontraditional fault currents and voltages during the fault. When these nontraditional fault quantities are observed, it is the hope of the authors that investigators will remember the techniques presented in this paper. Event analysis of neighboring devices can help provide a big-picture view of the system during the simultaneous fault. Phase and sequence quantities from neighboring devices in the system can give investigators clues such as missing current on certain phases in the case of a standing series fault. Further, a simple first-principles approach, such as KVL circuit analysis may be used to help gain insight and confidence in the findings from event analysis.

VIII. Acknowledgment

The authors would like to acknowledge and thank Bill Fleming and Cole Salo for their assistance in the initial analysis of this case study.

IX. References

[1] P. M. Anderson, *Analysis of Faulted Power Systems,* Iowa State Press, Ames, IA, 1973.

[2] J. Roberts and A. Guzmán, "Directional Element Design and Evolution," proceedings of the 21st Annual Western Protective Relay Conference, Spokane, WA, October 1994.

[3] K. Dase, S. Harmukh, and A. Chatterjee, "Detecting and Locating Broken Conductor Faults on High-Voltage Lines to Prevent Autoreclosing Onto Permanent Faults," proceedings of the 46th Annual Western Protective Relay Conference, Spokane, WA, October 2019.

[4] E. O. Schweitzer, III, and S. E. Zocholl, "Introduction to Symmetrical Components," proceedings of the 30th Annual Western Protective Relay Conference, Spokane, WA, October 2003.

[5] D. Tziouvaras, "Analysis of Complex Power System Faults and Operating Conditions," proceedings of the 35th Annual Western Protective Relay Conference, Spokane, WA, October 2008.

[6] S. Chase, S Sawai, and A. Kathe, "Analyzing Faulted Transmission Lines: Phase Components as an Alternative to Symmetrical

Components," proceedings of the 71st Annual Conference for Protective Relay Engineers, College Station, TX, 2018.

[7] S. E. Zocholl, "Three-Phase Circuit Analysis and the Mysterious k_0 Factor," proceedings of the 48th Annual Conference for Protective Relay Engineers, College Station, TX, April 1995.

X. BIOGRAPHIES

Eric Johnson obtained his electrical engineering undergraduate degree in 2007 from Clemson University. He began his technical career in 2008 with SCE&G (now Dominion Energy South Carolina) as a relay field engineer. The work involved distribution and transmission substations, distribution reclosers, underground switches, generating plants, and customer substations. He has been an engineer in relay applications since 2012 developing relay settings for distribution, transmission, and generation for all forms. He is currently heading up compliance for all PRC requirements. He is a member of the System Protection and Controls Working Group. He is currently a registered PE with the state of South Carolina.

Luke P. Booth is an application engineer with Schweitzer Engineering Laboratories, Inc. (SEL). He earned a BSEE degree from Georgia Institute of Technology in 2015, whereupon he joined Georgia Power as a protection and control field service engineer. He went on to join SEL in 2017 where he has been supporting customers across the Carolinas and Virginia. He is a registered professional engineer in the state of North Carolina.

Joe Perigo earned his BSEE and MSEE from Montana Technological University in 2016 and 2018, respectively. In June 2018, Joe joined Schweitzer Engineering Laboratories Inc. (SEL), where he works as a lead product engineer.